CFD MODELLING OF TWO-PHASE FLOW INSIDE GEOTHERMAL STEAM-WATER SEPARATORS

Munggang H. Purnanto[1], Sadiq J. Zarrouk[2*] and John E. Cater[2]

[1]Star Energy Geothermal (Wayang Windu) Ltd., Indonesia

[2] Department of Engineering Science, The University of Auckland, New Zealand

*s.zarrouk@auckland.ac.nz

Keywords: *Geothermal Separator, Cyclone, Computational Fluid Dynamics (CFD), Fluent.*

ABSTRACT

The steam-water separator is a vital component in liquid dominated geothermal steam field equipment. While various designs exist, the vertical cyclone separator dominates the design used worldwide. Most current designs are based on Bangma's experience in Wairakei in 1961, and Lazalde-Crabtree's (1984) empirical approach.

Although the design of a vertical cyclone separator is relatively simple, understanding of the fluid behaviour within the separator is still limited. Challenges arise from the difficulty in predicting the flow regime, pressure distribution and the separation efficiency inside the separator vessel. Due to this complexity, a numerical approach from Computational Fluid Dynamics (CFD) software is needed.

This paper simulates the two-phase fluid movement inside a geothermal cyclone separator using the Fluent® CFD software package. The inlet fluid characteristics were varied to see how the change in enthalpy and mass flow affected the cyclone separator performance. The effect of inlet shape design on separator performance was also studied. In order to model the swirling flow with a high degree of turbulence, as normally occurs inside the separator, the Renormalization Group (RNG) k-ε turbulence model was implemented. The separator efficiency was calculated by injecting liquid droplets after a converged solution was achieved. The Harwell technique was used to get an approximate estimate of the average liquid droplet size. The CFD simulation results demonstrated a promising method for optimizing the separator design.

1. INTRODUCTION

The steam-water separator is a vital component in liquid dominated geothermal steam field equipment. The separator enables the separation of steam and water from two-phase geothermal mixtures so that only dry steam is sent to run the turbine and generate electricity. While geothermal water usually has chloride and carbonates as dissolved components, the utilization of a separator will prevent water damage and scale deposition at turbine blades, hence, optimizing the long term energy conversion efficiency.

The majority of the well-known liquid-vapour separation process is performed using either knock out drums or demisting meshes (Hoffmann, 2007). However, each has its own limitations and can work for specific conditions only. Knock out drums work best for higher droplet loading while demisting meshes are suitable for low liquid loading in which the two phase slug condition does not exist (Hoffmann, 2007). Considering the nature of geothermal fluid, demisting meshes may not be suitable for geothermal applications.

Other well-known designs include the U-bend separator, the cyclone separator, and the horizontal separator. The U-bend separator works by a combination of centrifugal forces and gravity. It is able to remove up to 80 per cent of water. In earlier designs, the U-bend separator was usually installed in series with the cyclone separator to further increase its dryness (Figure 1). However, recent designs have excluded the U-bend separator because the cyclone itself is capable of removing almost all the water up to 95 per cent and above.

Figure 1: The U-bend Separator Installed Together with Top Outlet Cyclone Separator as seen in the Wairakei Field (Picture by Sadiq Zarrouk, 1997)

The cyclone type is the most popular due to its simple design, absence of moving parts, low cost, constant pressure drop, and high output quality and efficiency (Hoffmann, 2007; Lazalde-Crabtree, 1984). The inlet path is shaped in such a way so that the fluid enters the cyclone tangentially. As the fluid rotates, the liquid which has higher density will move downwards while the vapour which has lower density rises.

In initial designs, the steam was discharged at the top of the vessel while the brine was discharged at the bottom of the vessel. This type of separator is referred to as top outlet cyclone separator (TOC), also known as the Wood separator. It was designed by Merz and McLellan (Bangma, 1961) and is still in use in some of the geothermal bores at Wairakei (Figure 1).

The bottom outlet cyclone separator (BOC) superseded the TOC separator because it has a better efficiency. In this design, the steam pipe is placed inside the vessel and vapour exits from the bottom of the vessel. The challenge in designing the cyclone separator arises from the difficulties in prediction of the flow regime, pressure drop and the separation efficiency inside the vessel. Due to the

complexity of the geometry and flow, a numerical approach from Computational Fluid Dynamics (CFD) is required.

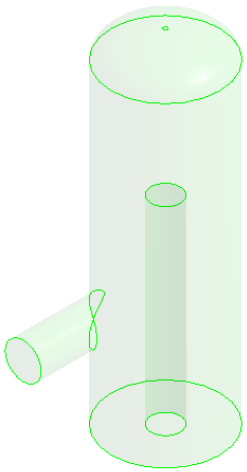

Figure 2: Separator Geometry based on Bangma (1961).

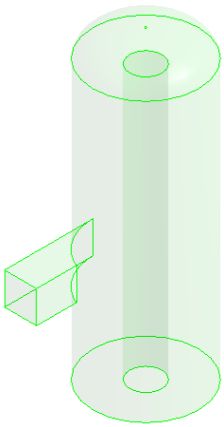

Figure 3: Separator Geometry based on Lazalde-Crabtree (1984).

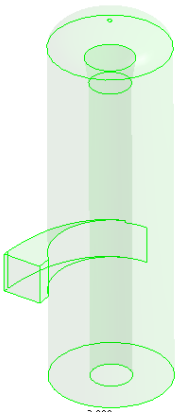

Figure 4: Separator Geometry based on the Spiral-Inlet Design.

Simple analytical and numerical solutions for predicting the flow within a geothermal separator have been presented by McKibbin (1998). McKibbin (1998) was able to show a simplified model for the flow of the steam phase inside the vessel to give the flow and pressure distribution patterns.

A study using CFD software for a geothermal vertical cyclone separator design has been performed by Pointon et al. (2009). Pointon et al. (2009) used a commercially available software package named Fluent, for their work (Fluent, 2010). They were able to show that CFD can be used to examine particular aspects of separator design, including upstream piping arrangements, separator geometric proportions, performance of large separators and enhancements to the entry to the steam outlet tube.

Following the successful study of Pointon et al. (2009), the present work simulated the two phase fluid movement inside a geothermal cyclone separator using Fluent. The separator dimensions were designed according to the approach from Bangma (1961) and Lazalde-Crabtree (1984) for typical geothermal fluid in a liquid dominated reservoir. Due to the natural flow inside the cyclone separator, which is swirling flow with a high degree of turbulence, a suitable turbulence model provided by Fluent was selected. Some simplifications to minimize the complexity of the model were made.

2. COMPUTATIONAL FLUID DYNAMICS

2.1 The Navier-Stokes Equation

The fluid motion is usually solved using the Navier-Stokes equation (Blazek, 2005). This equation is derived from the conservation of mass, the conservation of momentum and the conservation of energy. The general form of the Navier-Stokes equation within the boundary of $\partial\Omega$ and control volume Ω is given as follow (Blazek, 2005):

$$\frac{\partial}{\partial_t}\int_{\Omega} \vec{W}\,d\Omega + \oint_{\partial\Omega} \left(\vec{F_c} - \vec{F_v}\right) dS = \int_{\Omega} \vec{Q}\,d\Omega \qquad (1)$$

where $\vec{W}$ is the conservative variable, $\vec{F_c}$ is the flux vector related to the convective transport of quantities in the fluid, $\vec{F_v}$ is the flux vector that contains the viscous stresses as well as the heat diffusion, dS is the elemental surface area, $\vec{Q}$ is all volume sources due to body forces and volumetric heating.

2.2 Turbulence Models

Fluid flow inside the vertical cyclone separator is normally turbulent, indicated by the movement of the molecules in a strong chaotic fashion with complex irregular paths

Fluent's turbulent flow solver is based on the Reynolds-Average Navier-Stokes (RANS) equations (Fluent, 2010). These equations have the same form as the instantaneous Navier-Stokes equation with the velocities and other solution variables now represented as ensemble-averaged or time-averaged quantities.. A turbulence model is required to mimick the time averaged influence of the turbulence on the mean gas pattern.

There is no single turbulence model that reliably works for all conditions so different turbulence models have been proposed by different researchers in an attempt to solve for

the fluid behaviour inside a cyclone separator. The use of a Reynold Stress model (RSM) has been presented by Slack et al. (2000), Wang et al. (2003), Oliveira et al (2009), and Elsayed and Lacor (2010). The use of the Renormalization Group (RNG) k-ε model has been presented by Gimbun et al. (2005), Kefalas (2008), and Pointon et al. (2009). The use of Large Eddy Simulation (LES) has been presented by Slack et al. (2000), Schmidt et al. (2003), and Shalaby (2007). The use of the realizable k-ε turbulence model has been presented by Carmona et al. (2010)

The turbulence model in this work will use RNG k-ε model because it gives good prediction with less computational effort compared to the more complicated Reynold Stress Model (RSM) (Gimbun, 2005; Pointon et al., 2009). The RNG k-ε model is derived from the instantaneous Navier-Stokes equation using a statistical technique called renormalization group theory.

2.2 Two-Phase Model

Fluent provides two approaches for numerical calculation of multiphase flows: the Euler-Langrange approach and the Euler-Euler approach. The Euler-Langrange approach is used to model the discrete phase dispersed in the continuous phase. The fluid phase is treated as a continuum by solving the Navier-Stokes equations, while the dispersed phase is solved by tracking a large number of particles, bubbles or droplets through the calculated flow field. The dispersed phase can exchange momentum, mass and energy with the fluid phase. To use this approach, the dispersed second phase should be assumed to occupy a low volume fraction, usually less than 10-12 per cent, even though its mass loading may greatly exceed that value. This discrete phase model (DPM) will be used in this report to predict the separator efficiency.

The Euler-Euler approach treats the different phases as interpenetrating continua where the volume of one phase cannot be occupied by the other phase. The concept of volume fraction is introduced with an assumption that they are continuous functions of space and time having a sum equal to one. Fluent provides three different Euler-Euler multiphase models: the volume of fluid (VOF) model, the mixture model and the Eulerian model. The VOF model is appropriate for stratified or free-surface flows while the mixture and the Eulerian models are appropriate for flow where the dispersed-phase volume fractions exceed 10 per cent. For simpler problems, the mixture model is a better option than the Eulerian model because it solves a smaller number of equations and requires less computational effort. However, the accuracy of the mixture model is not as high as the Eulerian model.

The Stokes number (S_t) can be used to select the most appropriate model. The Stokes number is defined as the ratio between the particle relaxation time (τ_p) and the system response time (t_s). The particle relaxation time (τ_p) is defined by Eq. 2, while the system response time (t_s) is defined as the ratio between the characteristic length (L_s) and the characteristic velocity (V_s) of the system under investigation. If $S_t > 1$, either the DPM or Eulerian model is applicable. If $S_t < 1$, any of the DPM, mixture model or Eulerian model is applicable. Since the mixture model is the least expensive one, it should be selected as the first priority.

The Stokes number of a typical cyclone separator is much less than 1. Hence, the mixture model is selected as the most appropriate model to be used for the CFD modelling in this report.

$$\tau_p = \frac{\rho_p d_p^2}{18\mu_q} \tag{2}$$

where d_p is the particle diameter of secondary phase p and , μ_q is the viscosity of the other phase.

2.4 Boundary Condition

Fluent has ten boundary types to specify the fluid flow condition at the inlet and exit boundaries of the model. They are velocity inlet, pressure inlet, mass flow inlet, pressure outlet, pressure far-field, outflow, inlet vent, intake fan, outlet vent, and exhaust fan. Selection of the most appropriate boundary condition depends on which parameters are initially known. However, care should be taken when selecting the right combination, because the wrong boundary condition will result in the solution to a different problem.

Some boundary types may be advantageous over the other types for specific applications (Carmona et al., 2010). For example, a velocity inlet might be more preferable in incompressible flows than the mass flow inlet because at constant density the velocity inlet boundary condition will fix the mass flow. Another example, outflow boundary conditions are appropriate when the details of the flow velocity and pressure are not known prior to solution of the flow problem. However, they should not be used for compressible flow calculations. In the case of backflow, pressure outlet boundary condition should be used instead of outflow because it often results in a better rate of convergence during iteration.

2.4 Particle Tracking

A particle tracking method is required to predict the efficiency of the separator. This has been used by other researchers with the assumption that mist or mist-annular flow conditions exist at the upstream pipe feeding the separator (Hoffmann, 2007; Pointon et al., 2009; Shalaby, 2007). Separation efficiency is obtained by taking the ratio between the number of fine liquid droplets escaped from the steam outlet with the total number of liquid droplets at the two-phase inlet.

Particle tracking is performed by injecting liquid droplets and tracking their trajectories after a converged solution is achieved. Fluent's Discrete Phase Model (DPM) is used to perform the modelling. Fluent's prediction is based on the integration of the particle force balance equation which is written in a Langrangian reference frame (Fluent, 2010).

Considering that it is almost impossible to predict the flow behaviour and measure the droplet size distribution that is formed in the upstream pipe entering the separator, in this report, we used the Harwell technique to get a rough estimation of the average drop size. The Harwell procedure is one of several correlations available for computing drop

sizes and was developed on basis of steam-water, air-water and other fluid data (Hoffmann, 2007).

The Harwell equation calculates the Sauter mean droplet diameter as the mean of the surface distribution rather than the volume distribution according to the following formula (Hoffmann, 2007):

$$\langle x \rangle_{Sa} = 1.91 D_t \frac{Re^{0.1}}{We^{0.6}} \left(\frac{\rho_g}{\rho_l}\right)^{0.6} \quad (3)$$

where $\langle x \rangle_{Sa}$ is the Sauter mean droplet diameter, and Re and We are the Reynolds and Weber number, respectively. They are defined as,

$$Re = \frac{\rho_g v_t D_t}{\mu} \quad (4)$$

$$We = \frac{\rho_g v_t^2 D_t}{\sigma} \quad (5)$$

where D_t is the internal pipe diameter, ρ_g and ρ_l are the gas and liquid densities, μ_g is the gas viscosity, v_t is the mean gas velocity within the pipe and σ is the interfacial surface tension.

The volume-average (median) drop diameter is related to the Sauter-mean diameter through the following approximation:

$$\langle x \rangle_{med} = 1.42 x_{Sa} \quad (6)$$

The drop size distribution is plotted in Figure 5. From this distribution, about 5 per cent of the droplets will have the size of x/x_{med} = 0.3 or less and 100 per cent will be less than x/x_{med} = 2.9.

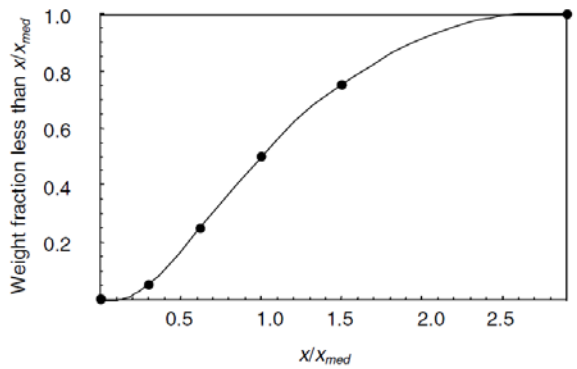

Figure 5: Standard Size Distribution for Droplets in Pipelines (Hoffmann, 2007).

3. CFD MODELLING PROCEDURES

3.1 Model Description

For the CFD modelling in this work, a typical single phase separator installation is assumed. The separator is fed by two wells producing two-phase fluid with the same flow and enthalpy. This configuration is assumed based on the typical condition normally found in a geothermal field. The fluid parameters are given in Table 1.

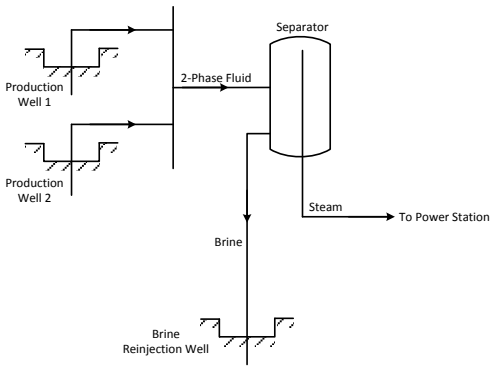

Figure 6: Schematic of the Model.

Table 1: Fluid Parameters.

Two phase flow from all wells ($\dot{m}_f$)	197.61	kg/s
Two phase enthalpy (h)	1600	kJ/kg
Separation pressure (P_{sep})	11.2	bara
T_{sat} at P_{sep}	184.85	°C
h_l at P_{sep}	784.66	kJ/kg
h_g at P_{sep}	2781.46	kJ/kg
ρ_l at P_{sep}	881.77	kg/m^3
ρ_g at P_{sep}	5.73	kg/m^3
μ_l at P_{sep}	145.96 × 10-6	kg/m.s
μ_g at P_{sep}	15.188 × 10-6	kg/m.s
Surface tension at P_{sep} (σ)	0.0411	N/m
$\dot{m}_l$ at P_{sep}	80.69	kg/s
$\dot{m}_g$ at P_{sep}	116.92	kg/s

Focus was given to the steady state condition of the two phase flow at the inlet and inside the vertical cyclone separator. The pre-separation process that occurs at the pipeline was not modelled. The flow of water to the brine pipe at the bottom of the vessel was also not modelled. The water level was assumed to be constant, located at just above the brine outlet pipe.

Several conditions that normally occur during operation of the power station were considered. They are given in Table 2.

Table 2: Fluid Data for Various Enthalpy Values at P_{sep} = 11.2 bara.

Mass flow rate two phase fluid $\dot{m}_f$ (kg/s) = 197.61 kg/s		
Conditions	Mass flow rate liquid $\dot{m}_l$ (kg/s)	Mass flow rate gas $\dot{m}_g$ (kg/s)
h = 1760 kJ/kg	101.09	96.52
h = 1680 kJ/kg	109	88.61
h = 1600 kJ/kg	116.92	80.69
h = 1520 kJ/kg	124.84	72.77
h = 1440 kJ/kg	132.76	64.85
h = 1600 kJ/kg, $\dot{m}_f$ decreases by 25%	87.69	60.52

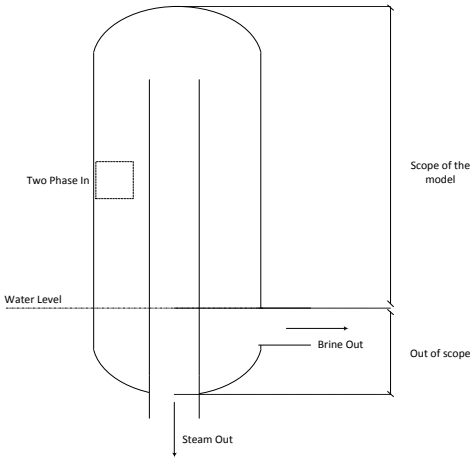

Figure 7: Scope of the Model.

The following assumptions are used in the present study:

a) The transition from the circular pipe into a rectangular inlet shape feeding the separator is designed to be smooth. The effect of improper piece placement is neglected.
b) The two phase flow is incompressible within the separator.
c) The two phase fluid at the inlet pipe is in mist form, where the gas phase is defined as the continuous primary phase while the liquid phase is defined as the dispersed secondary phase.
d) Liquid droplets are initially set to be uniform with average diameter of 10^{-5} m (10 μm).
e) No flashing occurs inside the separator.
f) The separation process occurs at an isothermal condition. Hence, the energy equation is not solved.
g) The relative atmospheric pressure is set to zero, so that the gauge pressure and the absolute pressure are equivalent.
h) The gravity force is acting downward along the vertical y-axis of the separator body with a magnitude of 9.81 m/s^2.
i) The wall roughness is equal to zero (smooth walls).

3.2 Geometry and Meshing

Three geometries were designed according to the approach from Bangma (1961) with circular tangential inlet shape, Lazalde-Crabtree (1984) with rectangular tangential inlet shape and typical current separator design used in the geothermal industry with a rectangular 90^o spiral inlet which was considered to be the optimum design combination of Bangma's approach and Lazalde-Crabtree's approach. For simplicity, the typical current design will be referred as the spiral-inlet design in this report. The vessel dimensions for each approach are given in Table 3. All vessel heads are considered to be 2:1 ellipses.

It should be noted that the top side of the middle steam tube of the spiral-inlet design forms a reverse truncated cone (Figure 4). Such a design was explained by Foong (2005) as a way to avoid a small thin water film clinging on the outside wall of the steam tube creeping up and falling into the steam outlet pipe.

All geometries were built using CAD Design Modeller. The Meshing Application was used to generate a computational mesh. Unstructured tetrahedron volumes were used for all geometries. Considering the size of the vessel, a number of nodes in the order of millions were preferable to provide a sufficiently fine mesh. To satisfy resolution requirements, an average element size of 5 cm was used. Some faces were set to have the element size of as small as 1 cm to avoid high gradients near boundaries.

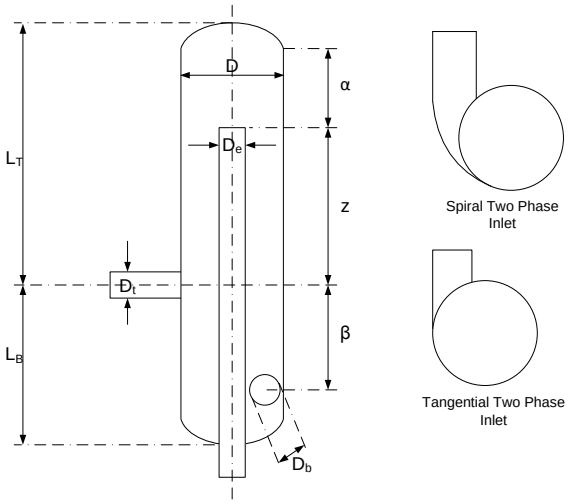

Figure 8: Vertical BOC Separator.

Table 3: Separator Vessel Dimension.

Parameter	Bangma Design		Lazalde-Crabtree Design		Spiral-Inlet Design	
	in meter	in D_t	in meter	in D_t	in meter	in D_t
D	2.172	3 D_t	2.389	3.3 D_t	2.134	2.95 D_t
D_e	0.579	0.8 D_t	0.724	1 D_t	0.724	1 D_t
D_b	0.724	1 D_t	0.724	1 D_t	0.508	0.7 D_t
α	2.353	3.25 D_t	0.109	0.15 D_t	0.2	0.28 D_t
β	2.172	3 D_t	2.534	3.5 D_t	2.320	3.2 D_t
Z	2.172	3D_t	3.982	5.5 D_t	4.195	5.8 D_t
L_T	5.068	7 D_t	4.688	6.475 D_t	4.929	6.8 D_t
L_B	3.258	4.5 D_t	3.602	4.975 D_t	3.579	4.9 D_t
A_o	0.4115 m^2		0.5242 m^2		0.5242 m^2	

3.3 Simulation Parameters

The mass flow inlet and the pressure outlet were used as the boundary conditions for the inlet and the outlet respectively. The inlet pressure was set at 11.4 bar while the outlet pressure was set at 11.2 bar.

A pressure-based approach was used for the solver because it is suitable for low speed incompressible flows (Fluent, 2010). The SIMPLE algorithm was used for the pressure-velocity coupling scheme. It is the default Fluent algorithm and able to give acceptable convergence results for most low speed problems.

Second order spatial differentiation was used to obtain a more accurate result. The Green-Gauss Node Based was used for gradients. The PRESTO (Pressure Staggering Option) was used for the pressure because it was suitable for flows with high swirl numbers. The Second Order Upwind scheme was used for the momentum, the turbulent kinetic energy and the turbulent dissipation rate. The Quick algorithm was used for the volume fraction.

An initial guess for the solution must be provided before starting the simulation. Care should be taken because the attained final solution sometimes depends on the initial guess. If the initial guess is close enough to the final result, the solver will do less work to reach the converged solution. Hybrid Initialization was used in this report because the user did not need to provide additional inputs for initialization and it might improve the convergence robustness for many cases.

4. CFD MODELLING RESULTS

4.1 Velocity Profile

The velocity vectors, coloured by velocity magnitude, for h = 1600 kJ/kg are shown in Figures 9 to 11. The vectors show the spiral movement when the fluid enters the separator body. Initially, the fluid enters the vessel at a paticular velocity and slightly accelerates before it starts to rotate. Then, the velocity decreases as the fluid starts to spin along the inner vessel wall. High velocity occurs at the outer wall of the vessel while lower velocity occurs at the centre of vessel.

An interesting pattern is observed in the spiral-inlet design. The fluid enters the separator in a smooth way such that the velocity magnitude inside the vessel is relatively uniform at the first rotation. High velocity rotation uniformly concentrates close to the outer wall, while slower velocity is uniformly concentrated in the centre. This condition is expected during the centrifuging process because the water will be forced to the outer vessel before it is affected by the steam stream in the centre of the cyclone that moves upward. Hence, the water will have a greater tendency to move downwards to be collected at the bottom of the separator.

The Bangma (1961) and Lazalde-Crabtree (1984) designs with tangential inlet shape shows different patterns, where there is a region near the outer wall which has lower velocity magnitude. This indicates that the transition from linear motion into rotation is not as smooth as observed in spiral inlet design. Disturbances may create atomization of the water as an impact of the main body of the water to the wall of the separator at a location opposite the inlet. This atomized water might be carried over by the steam, resulting in an increase of the steam wetness at the outlet of the separator.

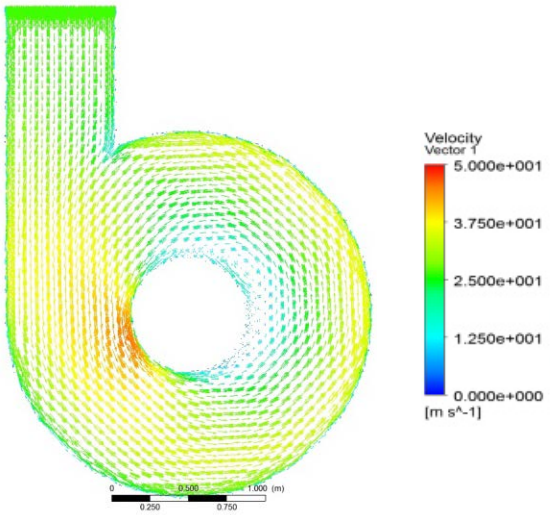

Figure 9: Velocity Profile for Bangma (1961).

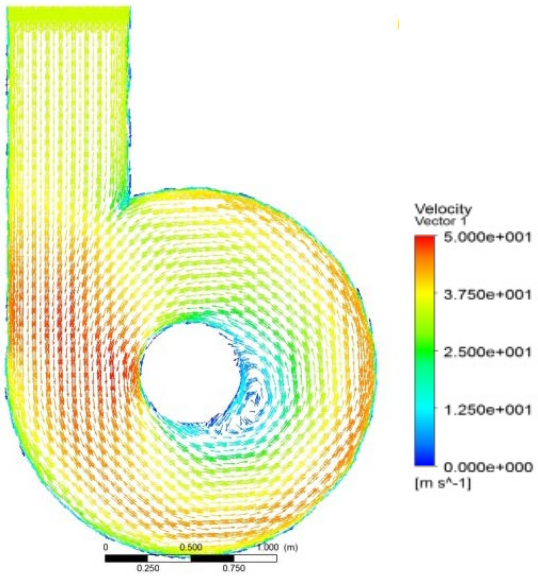

Figure 10: Velocity Profile for Lazalde-Crabtree (1984).

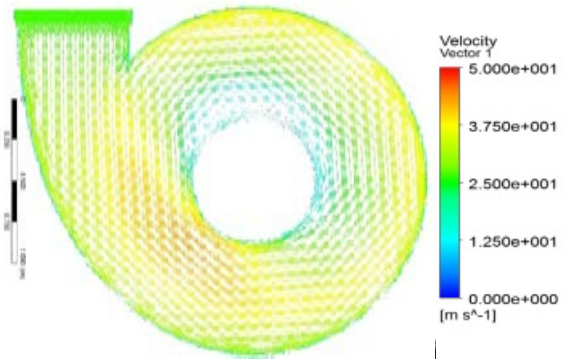

Figure 11: Velocity Profile for Spiral-Inlet Design.

In order to show quantitative results of the simulation, the velocity magnitudes for different fluid characteristics at certain heights of the vessel are plotted and compared as shown in Figures 12 to 14. The heights were measured as

the average distance between the inlet fluid and the outlet steam. The zero reference point was set at the top of the vessel.

For most conditions, the outer region has slightly higher velocity than the inner region. Generally, higher velocity is observed in the Bangma design, followed by the spiral-inlet design and then the Lazalde-Crabtree design. A similar pattern is also observed in solid-gas cyclone separators used in the chemical industry (Singh et al., 2006; Wang et al., 2003). However, some conditions are the other way around. This indicates that the velocity magnitude is not distributed uniformly. Further analysis requires validation using measurements.

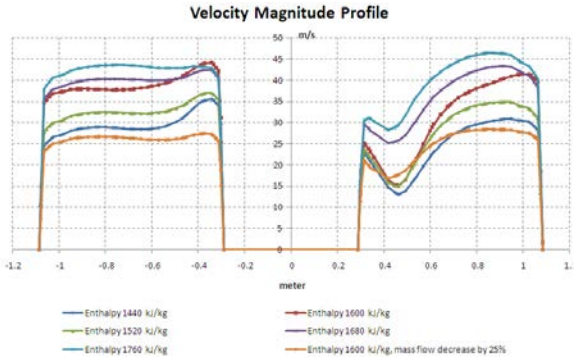

Figure 12: Bangma at y = -2.85m.

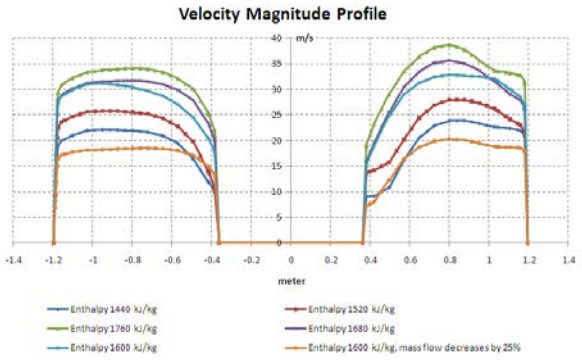

Figure 13: Lazalde-Crabtree at y = -2.04m.

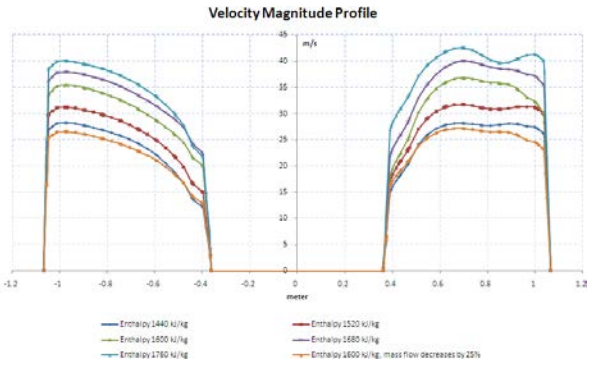

Figure 14: Spiral-Inlet Design at y = -3.31m.

4.2 Pressure Distribution

Figures 15 to 17 show the pressure distribution inside the separator for various inlet fluid enthalpy in each design. Uniform patterns are found. Lower pressure is observed in the centre of the separator, while higher pressure is observed at the outer wall. This is due to the influence of cyclonic flow and the centripetal acceleration induced by the rotation (McKibbin, 1998). The advantage of this condition is that more flash may occur because of the pressure is lower than the saturation value, creating a much drier steam at the outlet of the separator.

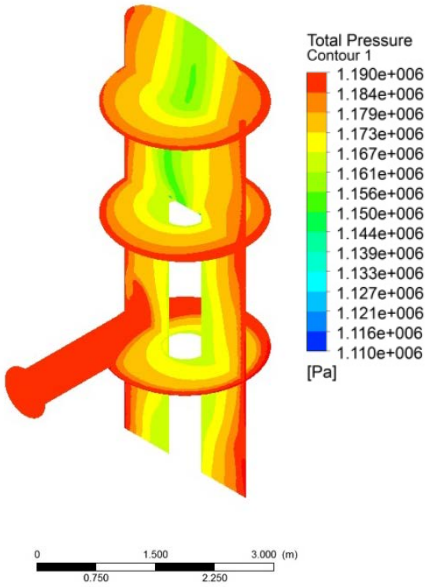

Figure 15: Bangma, h = 1760 kJ/kg.

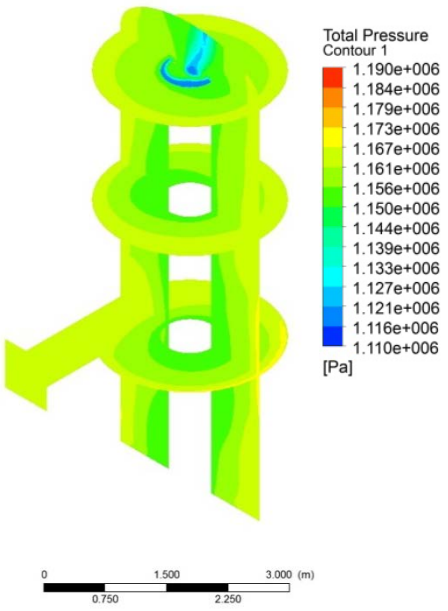

Figure 16: Lazalde-Crabtree, h = 1760 kJ/kg.

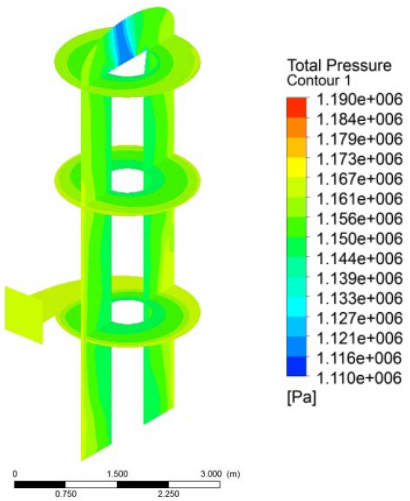

Figure 17: Spiral-Inlet Design, h = 1760 kJ/kg.

4.3 Outlet Steam Quality

The strategy for predicting the outlet steam quality of the separator was to inject a large number of particles at the inlet. The particles sizes were calculated using the Harwell technique (Figure 5) and were considered to be uniformly distributed at the inlet surface. Injections were carried out nine times. Each injection used a different droplet diameter.

Although the number of injected particles for each cycle was the same, they represented different mass flow. The steam output quality was calculated as the mass flow ratio of the separated steam with the total steam-water that left from the outlet. Any droplets that reached the bottom of separator were considered to be perfectly separated.

During injection, a particle was assumed to be smooth. The maximum number of Euler time steps of 10^5 was set. After injection, there were three conditions of particles: trapped, escaped and incomplete. Trapped particles are the liquid droplets that are separated, escaped particles have been carried over to the steam outlet, while the incomplete particles have exceeded the maximum number of steps and Fluent abandoned the trajectory calculation. The incomplete particles made the interpretation process difficult because they might be either trapped or escaped. Increasing the maximum number of steps to be 10^6 did not significantly decrease the number of incomplete particles.

In order to cope with this problem, a possible approach was to assume that the incomplete particles were all separated. Although this approach might not be very rigorous, it did provide the most promising collection efficiency estimates, close to the result from the empirical method developed by Lazalde-Crabtree (1984).

Figures 18 to 20 show the differences between modelling and calculation, and how the change in enthalpy and mass flow affect the outlet steam quality. The Lazalde-Crabtree's data (1984) that correlate the inlet steam velocity and the outlet steam quality are also plotted. These data were taken from several Webre separators at different geothermal fields and they were intended to show the general patterns that observed in actual condition (green line).

The lowest inlet velocity corresponds to a condition when the inlet enthalpy is 1600 kJ/kg and the inlet mass flow decreases by 25 per cent. The highest inlet velocity corresponds to a condition when the enthalpy is 1760 kJ/kg. The remaining cases are located between these two values; a low velocity value is at the left hand side while a high value is at the right hand side.

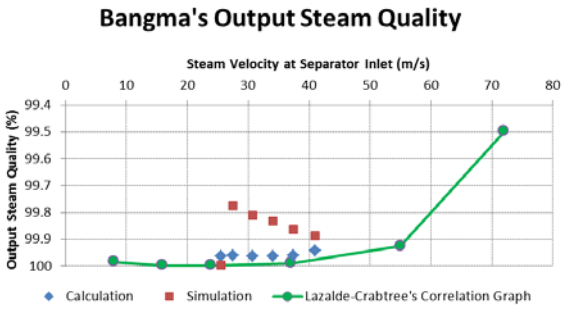

Figure 18: Outlet Steam Quality against Inlet Velocity.

In Bangma's design, the difference between calculation and simulation varies between 0.03 per cent up to 0.18 per cent. Figure 18 shows that the outlet steam quality increases as the inlet enthalpy increases. High outlet steam quality is also observed when the enthalpy remains the same (1600 kJ/kg) but the mass flow decreases. The simulation patterns do not follow the patterns from calculation and Lazalde-Crabtree's recorded data. However, their values are still within a reasonable range.

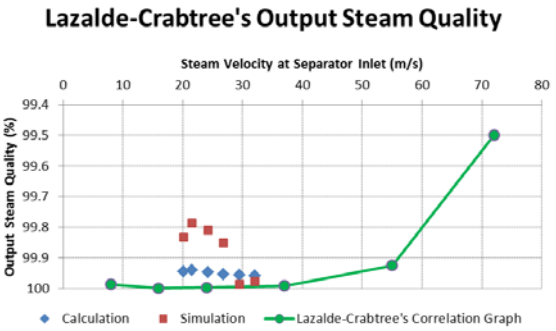

Figure 19: Outlet Steam Quality against Inlet Velocity.

In Lazalde-Crabtree's design, the difference between calculation and simulation varies between 0.02 per cent up to 0.15 per cent. Similar to Bangma's, the output steam quality increases as the enthalpy and velocity increases (Figure 19). The highest output quality is observed when the enthalpy is 1680 kJ/kg and the inlet velocity is 29.48 m/s. Increasing the enthalpy further will cause a slight decrease in the output steam quality.

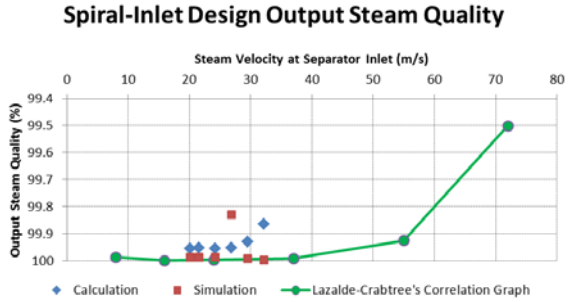

Figure 20: Outlet Steam Quality against Inlet Velocity.

In the spiral-inlet design (Figure 20), the difference between simulation and calculation varies between 0.03 per cent up to 0.13 per cent. Unexpected behaviour is observed when the enthalpy is 1600 kJ/kg and the inlet velocity is 26.81 m/s. The outlet steam quality does not follow the pattern where the quality should increase as the inlet velocity increases. The cause of this behaviour is unknown and should be further investigated.

5. CONCLUSIONS

1) The predicted performance of CFD simulation is in good agreement with the Lazalde-Crabtree empirical approach. The Fluent RNG k-ε turbulence model is good enough to be used as a first attempt for CFD analysis.
2) The CFD analysis was able to visualize the two-phase behaviour inside the separator, a feature that cannot be achieved from the empirical approach. The pressure distribution patterns and velocity profiles agree well with the existing theory.
3) The CFD modelling was able to show how different geometry, different inlet shapes and different inlet fluid characteristics affect the separator performance. These results indicate that CFD is a promising tool which can be used to optimize the separator design that meets the operating requirements at low cost.
4) Experimental work is required to calibrate the result of the present CFD modelling in order to have more confidence in the results.

REFERENCES

Bangma, P.: The Development and Performance of a Steam-Water Separator for Use on Geothermal Bores. *Proceedings of the U.N. Conference on New Sources of Energy Rome 1961*, Vol. 3(Issue G/13): pp. 60 – 77. (1961).

Blazek, J.,: Computational Fluid Dyanamics: Principles and Applications Second Edition. Elsevier Ltd., Great Britain. (2005).

Carmona, M., Cortes, C. and Ramirez, A.: A Numerical Study of the Flow in a Cyclone Separator Using the k-ε Realizable Turbulence Model. In: J.C.F. Pereira, Sequeira, A. (Editor), *V European Conference on Computational Fluid Dynamics*, Lisbon, Portugal. (2010).

Elsayed, K. and Lacor, C.: Optimization of the Cyclone Separator Geometry for Minimum Pressure Drop using Mathematical Models and CFD Simulations. Chemical Engineering Science, Vol. 65: 6048 - 6058. (2010).

Fluent: Ansys Fluent Theory Guide Release 13.0. Ansys, United States of America. (2010).

Foong, K.C.: Design Concept for a More Efficient Steam-Water Separator, *Proceedings World Geothermal Congress*, Antalya, Turkey. (2005).

Gimbun, J., Chuah, T.G., Fakhru'l-Razi, A. and Choong, T.S.Y.: The Influence of Temperature and Inlet Velocity on Cyclone Pressure Drop: A CFD Study. Chemical Engineering and Processing, Vol. 44: pp. 7 - 12. (2005).

Hoffmann, A.C. and Stein, L.E.: Gas Cyclones and Swirls Tubes Principles, Design and Operation 2nd Edition. Springer, New York. (2007).

Kefalas, P.I. and Margaris, D.P.: Numerical Analysis of Fluid Flow in a Compact Phase Separator. The Open Mechanical Engineering Journal: pp. 21-31. (2008).

Lazalde-Crabtree, H.: Design Approach of Steam-Water Separators and Steam Dryers for Geothermal Applications. Geothermal Resources Council Bulletin(September): 11 – 20. (1984).

McKibbin, R.: Fluid Flow in a Flashing Cyclone Separator., *Proceedings 20th NZ Geothermal Workshop*, New Zealand. (1998).

Oliveira, D.C., Almeida, C.A.K., Vieira, L.G.M., Damasceno, J.J.R. and Barrozo, M.A.S.: Influence of Geometric Dimensions on the Performance of a Filtering Hydrocyclone: An Experimental and CFD Study. Brazilian Journal of Chemical Engineering, Vol. 26(No. 03): pp. 575 - 582. (2009).

Pointon, A.R., Mills, T.D., Seil, G.J. and Zhang, Q.: Computational Fluid Dynamic Techniques for Validating Geothermal Separator Sizing. GRC Transactions, Vol. 33: pp. 943 - 948. (2009).

Schmidt, S., Blackburn, H.M., Rudman, M. and Sutalo, I.: Simulation of Turbulent Flow in Cyclonic Separator, Third International Conference on CFD in the Minerals and Process Industries, Melbourne, Australia. (2003).

Shalaby, H.H.: On the Potential of Large Eddy Simulation to Simulate Cyclone Separators, Chemnitz University of Technology, Chemnitz, Germany, 121 pp. (2007).

Singh, V., Srivastava, S., Chaval, R., Vitankar, V., Basu, B. and Agrawal, M.C.: Simulation of Gas-Solid Flow and Design Modifications of Cement Plant Cyclones, *Fifth International Conference on CFD in the Process Industries*, CSIRO, Melbourne, Australia. (2006).

Slack, M.D., Prasad, R.O., Bakker, A. and Boysan, F.: Advances in Cyclone Modelling Using Unstructured Grids. TransIChemE, Vol. 78 Part A: page 1098 - 1104. (2000).

Wang, B., Xu, D.L., Xiao, G.X., Chu, K.W. and Yu, A.B.: Numerical Study of Gas Solid Flow in a Cyclone Separator, *Third International Conference on CFD in the Minerals and Process Industries*, Melbourne, Australia. (2003).